J Sci Comput
DOI 10.1007/s10915-017-0423-x

Fast Laplace Transform Methods for Free-Boundary Problems of Fractional Diffusion Equations

Zhiqiang Zhou[1] · **Jingtang Ma**[1] · **Hai-wei Sun**[2]

Received: 27 November 2016 / Revised: 9 March 2017 / Accepted: 20 March 2017

Abstract In this paper we develop a fast Laplace transform method for solving a class of free-boundary fractional diffusion equations arising in the American option pricing. Instead of using the time-stepping methods, we develop the Laplace transform methods for solving the free-boundary fractional diffusion equations. By approximating the free boundary, the Laplace transform is taken on a fixed space region to replace discretizing the temporal variable. The hyperbola contour integral method is exploited to restore the option values. Meanwhile, the coefficient matrix has theoretically proven to be sectorial. Therefore, the highly accurate approximation by the fast Laplace transform method is guaranteed. The numerical results confirm that the proposed method outperforms the full finite difference methods in regard to the accuracy and complexity.

Keywords American option pricing · Free-boundary problems · Fractional diffusion equations · Laplace transform methods · Hyperbola contour integral · Toeplitz matrix

Mathematics Subject Classification 35S15 · 65F10 · 65M06 · 91G20 · 91G60

The work was supported by National Natural Science Foundation of China (Grant No. 11671323), Program for New Century Excellent Talents in University (Grant No. NCET-12-0922) and the Fundamental Research Funds for the Central Universities (Grant No. 15CX141110). It was also partially supported by Research Grants MYRG2016-00063-FST from University of Macau and 054/2015/A2 from FDCT of Macao.

✉ Jingtang Ma
mjt@swufe.edu.cn

Zhiqiang Zhou
zqzhou@2014.swufe.edu.cn

Hai-wei Sun
HSun@umac.mo

1 School of Economic Mathematics, Southwestern University of Finance and Economics, Wenjiang, Chengdu 611130, People's Republic of China

2 Department of Mathematics, University of Macau, Taipa, Macau

1 Introduction

The finite moment log stable model assume the logarithm value of the underlying $x_t = \log S_t$ follows a stochastic differential equation (SDE) of the maximally skewed log stable process [5]:

$$dx_t = (r - \nu)dt + \sigma dL_t^{\alpha,-1}, \tag{1}$$

where r is the risk free interest rate and $\nu = -\frac{1}{2}\sigma^\alpha \sec\frac{\alpha\pi}{2}$ is a convexity adjustment, $L_t^{\alpha,-1}$ denotes the maximally skewed log stable process, which is a special case of the Lévy-α-stable process $L_t^{\alpha,\beta}$ with $\alpha \in (1, 2)$ as the tail index and $\beta = -1$ as the skewed index. With this SDE, the classical option pricing Black–Scholes–Merton PDE becomes a so-called fractional partial differential equation (FPDE) with respect to logarithm value $x = \log S$.

Let $V(x, \tau)$ be the price of American put option and let $\tau = T - t$ represent the remaining date to expire time T. Then $V(x, \tau)$ satisfies the following FPDEs (see Chen et al. [7]):

$$\frac{\partial V}{\partial \tau} = \nu\, {}_{-\infty}D_x^\alpha V + (r - \nu)\frac{\partial V}{\partial x} - rV, \quad x \in (x_f(\tau), +\infty),\ \tau \in (0, +\infty), \tag{2}$$

in which $\alpha \in (1, 2)$, initial condition

$$V(x, 0) = (K - e^x)^+, \quad x \in (-\infty, +\infty), \tag{3}$$

and boundary conditions

$$V(x, \tau) = K - e^x, \quad \tau \in [0, +\infty),\ x \le x_f(\tau), \tag{4}$$

$$\frac{\partial V(x, \tau)}{\partial x} = -e^x, \quad \tau \in [0, +\infty),\ x \le x_f(\tau), \tag{5}$$

$$\lim_{x\to+\infty} V(x, \tau) = 0, \quad \tau \in [0, +\infty), \tag{6}$$

where $(y)^+ = \max(y, 0)$, K is the strike price, $x_f(\tau)$ is the early exercise boundary which is unknown and should be calculated in later calculation. The fractional derivative ${}_{-\infty}D_x^\alpha V(x, \tau)$ is taken as Grünwald–Letnikov formula

$${}_{-\infty}D_x^\alpha V(x, \tau) = \lim_{x_0\to-\infty} {}_{x_0}D_x^\alpha V(x, \tau) := \lim_{x_0\to-\infty} \left(\lim_{\substack{h\to 0 \\ nh = x - x_0}} \frac{1}{h^\alpha} \sum_{k=0}^{n} g_k^{(\alpha)} V(x - kh, \tau) \right), \tag{7}$$

where

$$g_0^{(\alpha)} = 1, \quad g_k^{(\alpha)} = (-1)^k \frac{\alpha(\alpha - 1)\dots(\alpha - k + 1)}{k!} \ \text{ for } k \ge 0. \tag{8}$$

We note that there is the recurrence relationship

$$g_0^{(\alpha)} = 1, \quad g_k^{(\alpha)} = \left(1 - \frac{\alpha + 1}{k}\right) g_{k-1}^{(\alpha)}, \tag{9}$$

which can be used to simplify the computation of $g_k^{(\alpha)}$. Note that there are other two common definitions of fractional derivatives: Riemann–Louville and Caputo fractional derivatives. They are equivalent to Grünwald–Letnikov formula when the lower limits in the integrals are taken as $-\infty$ (see [26]).

Applying the Laplace transform to the above FPDEs with respect to time variable leads to a fractional ordinary differential equation (FODE) parameterized by the Laplace mode. Mathematically the solution to the FPDEs can be represented as a contour integral form in the complex plane, which is the Laplace inversion for the solution of the FODEs. A quadrature rule to a contour integral should be developed, where for each quadrature point the FODEs have to be solved to determine the value of the integrand. This approach is normally named as contour integral method or Laplace transform method. The convergence of the Laplace transform method is controlled by the number of space mesh N and the parameter L for the numerical Laplace inversion. The convergence rate in L for the Laplace transform methods is analogous to that in the time-step size for the time-stepping methods, and the convergence rate in N is the same as the corresponding full finite difference methods. The Laplace transform method has exponentially decaying convergence in L. Therefore the Laplace transform methods are much faster than the time-stepping methods. Sheen et al. [29,30] introduce this idea for parabolic equations. The methods are later developed and improved in a number of papers: McLean et al. [18], McLean and Thomée [19–21], Weideman [34], Lee et al. [15]. Pang and Sun [24] develop the method for solving fractional diffusion equations. All the work is for the fixed-boundary problems. For the free-boundary problems, there will be challenges in getting the contour integral representation with Laplace transforms and developing the fast quadrature rules for the Laplace inversion.

There are also many applications of the methods in mathematical finance (see [1–4,7,9,11, 13,14,25,28]). All the work is for option pricing without early exercise features. A number of papers have tried to develop the Laplace transform methods to the option pricing with early exercise features. A simple framework for Laplace transform methods is introduced by Zhu [38] for pricing American options under GBM models. This framework is later developed for evaluation of finite-lived Russian options by Kimura [12], pricing American options under CEV models by Pan and Wong [27] and Wong and Zhao [36], pricing American options under hyper-exponential jump-diffusion model by Leippold and Vasiljević [17]. But this framework makes use of the assumption that early exercise boundary (free-boundary) moves very slowly in comparison with the "diffusion" of the option price. But the free boundary changes considerably at time close to $\tau = 0$. Therefore the assumption is not reasonable and causes large errors in the computations.

In this paper, we develop a Laplace transform method for solving the FPDEs from American option pricing. The FPDEs defined on the moving region $[x_f(\tau), +\infty)$ is modified as a new form on the fixed region which contains the unknown free boundary $x_f(\tau)$. Then performing the Laplace transform leads to an FODE which involves the inverse function $\tau_f(x)$ of function $x_f(\tau)$. Using the finite difference method combined with the approximation of the function $\tau_f(x)$, where the optimal parameters of the approximation is obtained by minimizing the prescribed residual error, we obtain the numerical solution of the FODE in the Laplace space. Lastly, we develop the contour integral methods to compute the Laplace inversion. Numerical examples are carried out to confirm that this new Laplace transform method is rather accurate and reliable.

The remaining parts of this paper are arranged as follows: In Sect. 2, we develop finite difference methods (FDMs) to solve the American option pricing problems with fractional diffusion equations. In Sect. 3, a new Laplace transform method is proposed. In Sect. 4, the analysis of contour integral method for Laplace inversion is carried out. In Sect. 5, numerical examples are provided to compare the LTMs with the FDMs. Conclusions are given in the final section.

2 Finite Difference Methods

We now describe a FDM to solve the FPDEs (2) with initial condition (3) and boundary conditions (4)–(6). Using the FDM we will show that the early exercise boundary $x_f(\tau)$ decreases strictly as τ increasing by numerical computations with different parameters α and σ. The monotonicity of $x_f(\tau)$ plays an important role in the Laplace transform methods. Moreover, we will compare the Laplace transform methods with the FDMs.

Assume $0 \le x_L \ll x_f(\tau)$ and x_R is a sufficiently large number such that $V(x_R, \tau) = 0$ for all $\tau \in (0, \infty)$. Define $\Delta\tau = T/M$, $\Delta x = (x_R - x_L)/(N+1)$ and uniform time mesh and space mesh

$$\tau_j = j\Delta\tau, \quad j = 0, 1, \ldots, M; \tag{10}$$

$$x_i = x_L + i\Delta x, \quad i = 0, 1, \ldots, N+1. \tag{11}$$

Assume $x_f(\tau_j) \approx x_p$ for a certain integer number $1 \le p = p(j) \le N$ and denote $V_i^j = V(x_i, \tau_j)$. Using the shifted Grünwald–Letnikov approximation (see [22,23]) for $i > p$, the fractional derivative is discretized by

$$\begin{aligned} -{}_{-\infty}D_x^\alpha V(x,\tau_j)\big|_{x=x_i} &\approx {}_{x_L}D_x^\alpha V(x,\tau_j)\big|_{x=x_i} \\ &\approx \frac{1}{\Delta x^\alpha}\sum_{k=0}^{i-p} g_k^{(\alpha)} V_{i+1-k}^j + \frac{1}{\Delta x^\alpha}\sum_{k=i+1-p}^{i+1} g_k^{(\alpha)} V_{i+1-k}^j \\ &= \frac{1}{\Delta x^\alpha}\sum_{k=0}^{i-p} g_k^{(\alpha)} V_{i+1-k}^j + \frac{1}{\Delta x^\alpha}\sum_{k=i+1-p}^{i+1} g_k^{(\alpha)} (K - e^{x_{i+1-k}}). \end{aligned} \tag{12}$$

Inserting (12) and the first order difference expressions

$$\frac{\partial V(x_i,\tau)}{\partial\tau}\Big|_{\tau=\tau_j} \approx \frac{V_i^j - V_i^{j-1}}{\Delta\tau}, \quad \frac{\partial V(x,\tau_j)}{\partial x}\Big|_{x=x_i} \approx \frac{V_{i+1}^j - V_{i-1}^j}{2\Delta x} \tag{13}$$

into (2), and using the boundary conditions (4) and (6), we obtain the following linear system of equations

$$\mathbf{A}^{(p)}\mathbf{v}^{(j,p)} = \mathbf{b}^{(j,p)}, \tag{14}$$

where

$$\mathbf{A}^{(p)} = \mathbf{D} - \frac{\nu\Delta\tau}{\Delta x^\alpha}\mathbf{G}_{\alpha,p}, \quad \mathbf{v}^{(j,p)} = \left[V_{p+1}^j, V_{p+2}^j, \ldots, V_N^j\right]^\mathsf{T}, \tag{15}$$

$$\mathbf{b}^{(j,p)} = \left[V_i^{j-1} - \frac{\nu\Delta\tau}{\Delta x^\alpha}\sum_{k=i+1-p}^{i+1} g_k^{(\alpha)}(K - e^{x_{i+1-k}}) - b(K - e^{x_p})\mathbf{1}_{\{i=p+1\}}\right]^\mathsf{T}_{i=p+1,\ldots,N}. \tag{16}$$

Note that $b(K - e^{x_p})\mathbf{1}_{\{i=p+1\}}$ in equation (16) comes from the left boundary $V(x_p, \tau_j) = K - e^{x_p}$. Here, both $\mathbf{D}$ and $\mathbf{G}_{\alpha,p}$ are $(N-p) \times (N-p)$ matrices

$$\mathbf{D} = \begin{bmatrix} a & -b & & & \\ b & a & -b & & \\ & \ddots & \ddots & \ddots & \\ & & b & a & -b \\ & & & b & a \end{bmatrix}, \quad \mathbf{G}_{\alpha,p} = \begin{bmatrix} g_1^{(\alpha)} & g_0^{(\alpha)} & & & \\ g_2^{(\alpha)} & g_1^{(\alpha)} & g_0^{(\alpha)} & & \\ \vdots & \ddots & \ddots & \ddots & \\ g_{N-p-1}^{(\alpha)} & \cdots & g_2^{(\alpha)} & g_1^{(\alpha)} & g_0^{(\alpha)} \\ g_{N-p}^{(\alpha)} & \cdots & g_3^{(\alpha)} & g_2^{(\alpha)} & g_1^{(\alpha)} \end{bmatrix}, \tag{17}$$

where

$$a = 1 + r\Delta\tau, \quad b = \frac{(r-\nu)\Delta\tau}{2\Delta x}.$$

Finally we need to determine the index $p = p(j)$ such that $x_f(\tau_j) \approx x_p$. This can be done by matching the boundary condition (5) and searching with the secant method such that

$$\frac{V_{p+1}^j - V_{p-1}^j}{2\Delta x} \approx \frac{\partial V(x_p, \tau_j)}{\partial x} = -e^{x_p}.$$

The computational procedure is summarized in the following Algorithm 1.

Algorithm 1 FDM for solving (2)

1: **Step 1.** Let $x_{p(0)} = \log K$ and $V_i^0 = \max(K - e^{x_i}, 0)$ for $i = 0, 1, \ldots, N$.
2: **Step 2.** Solving early exercise boundary and option price by time-stepping:
3: **for** $j = 1, 2, \ldots, M$ **do**
4: Let $p_L = 1$, $p_R = N$.
5: **while** $p_L < p_R - 1$ **do**
6: Let $p = \text{floor}[(p_L + p_R)/2]$;
7: Solve Eq. (14);
8: If $\frac{V_{p+1}^j - V_{p-1}^j}{2\Delta x} > -e^{x_p}$, let $p_R = p$;
9: If $\frac{V_{p+1}^j - V_{p-1}^j}{2\Delta x} \le -e^{x_p}$, let $p_L = p$.
10: **end while**
11: Save $p(j) = p$ and $\mathbf{v}^{(j,p)}$.
12: **end for**
13: **Step 3.** Output the free boundary $x_{p(j)}$ and option values $\mathbf{v}^{(j,p)}$ for different time index j.

Figure 1 plots the free boundaries $x_f(\tau)$ with different values of α and σ. It can be observed from Fig. 1 that $x_f(\tau)$ is strictly decreasing and convex on the interval $[0, +\infty)$. For the model with $\alpha = 2$ (integer diffusion equations), it has been proved by [8,37] that the free-boundary function $x_f(\tau)$ of American puts is continuously differentiable, strictly decreasing and convex on the interval $[0, +\infty)$.

3 Laplace Transform Methods

Denote $\overline{x} = x_f(0+) = \log K$ the boundary at expire date T. Let $\underline{x} = x_f(+\infty)$ be the boundary of perpetual American option. Then it satisfies the following FODE:

$$\nu_{-\infty} D_x^{\alpha} V^{\infty}(x) + (r - \nu)\frac{\partial V^{\infty}(x)}{\partial x} - rV^{\infty}(x) = 0, \quad x \in (\underline{x}, +\infty), \tag{18}$$

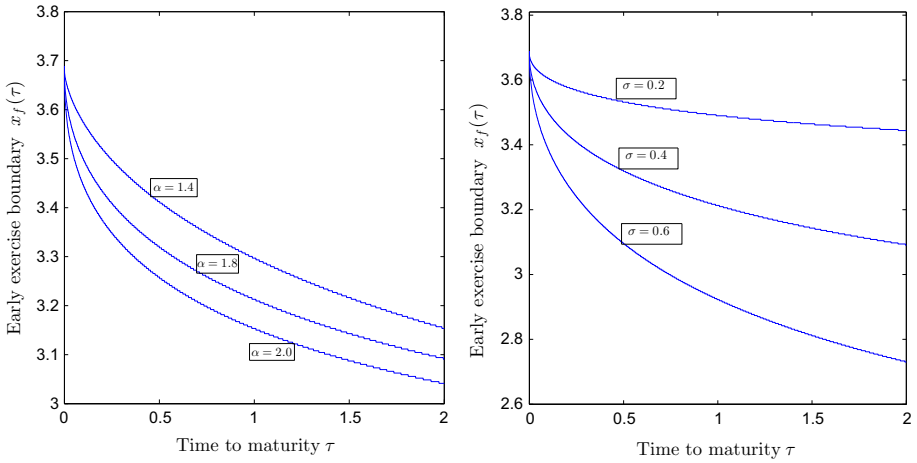

Fig. 1 Early exercise boundaries obtained by the FDMs with parameters: $T = 2$, $r = 0.05$, $K = 40$, $N = 8000$, $M = 8000$. *Left figures* are for different values of α with fixed $\sigma = 0.4$; *Right figures* for different values of σ with fixed $\alpha = 1.8$

with boundary conditions:

$$V^{\infty}(x) = K - e^{x}, \quad x \le \underline{x}, \tag{19}$$

$$\frac{\partial V^{\infty}(x)}{\partial x} = -e^{x}, \quad x \le \underline{x}, \tag{20}$$

$$\lim_{x \to +\infty} V^{\infty}(x) = 0. \tag{21}$$

The early exercise boundary $\underline{x}$ can be searched by the secant method in the region $[0, \overline{x}]$ such that (19), (20) and (21) hold true.

Assume $x_L \ll \underline{x}$ such that ${}_{-\infty}D_x^{\alpha} V^{\infty} \approx {}_{x_L}D_x^{\alpha} V^{\infty}$ and x_R is sufficiently large such that $V^{\infty}(x_R) \approx 0$. Define

$$\Delta x = (x_R - x_L)/(N+1), \tag{22}$$

$$x_i = x_L + i\,\Delta x, \quad i = 0, 1, \ldots, N+1. \tag{23}$$

Assume $\underline{x} \approx x_p$, for some index $0 < p < N+1$. Denote $V_i^{\infty} \approx V^{\infty}(x_i)$. Then the FDM for FODE (18) is given by

$$\frac{\nu}{(\Delta x)^{\alpha}} \sum_{k=0}^{i-p} g_k^{(\alpha)} V_{i+1-k}^{\infty} + \frac{\nu}{(\Delta x)^{\alpha}} \sum_{k=i+1-p}^{i+1} g_k^{(\alpha)} (K - e^{x_{i+1-k}}) + (r-\nu)\frac{V_{i+1}^{\infty} - V_{i-1}^{\infty}}{2\Delta x} - r V_i^{\infty} = 0, \quad i = p+1, p+2, \ldots, N. \tag{24}$$

To search $\underline{x}$ we solve Eq. (24) with boundary conditions (19) and (21) and find index p such that $x = x_p$ satisfies condition (20) by secant method. The detailed computational procedure is summarized as Algorithm 2.

Theorem 1 *With the same initial condition* (3) *and boundary conditions* (4)–(6)*, the FPDE* (2) *is equivalent to the following FPDE:*

Algorithm 2 Compute early exercise boundary $\underline{x} = x_f(\infty)$ for perpetual American put

Step 1. Let $L = 1$, $H = p_*$ such that $x_{p_*} \approx \log K$.
Step 2. Using secant method to search x_p:
while $L < H - 1$ **do**
  Let $p = \text{floor}[0.5(L + H)]$.
  Let $V_k^\infty = K - e^{x_k}$, $(k = 0, 1, \ldots, p)$, $V_{N+1}^\infty = 0$ and solve Eq. (24).
  % Verify the boundary condition (20):
  if $\frac{V_{p+1}^\infty - V_{p-1}^\infty}{2\Delta x} < -e^{x_p}$ **then**
    update $L = p$;
  else
    update $H = p$.
  end if
end while
Step 3. Output $\underline{x} = x_p$.

$$\frac{\partial V}{\partial \tau} = \nu_{-\infty} D_x^\alpha V + (r - \nu)\frac{\partial V}{\partial x} - rV + rK\mathbf{1}_{\{x \le x_f(\tau)\}}, \quad x \in (\underline{x}, +\infty), \ \tau \in (0, +\infty), \tag{25}$$

where $\mathbf{1}_{\{x \le x_f(\tau)\}}$ *is the indicator function.*

Proof On the region $\tau \in (0, \infty)$, $x \in (\underline{x}, x_f(\tau))$, we know from the boundary condition (4) that $V(x, \tau) = K - e^x$. Direct calculation shows that $V(x, \tau) = K - e^x$ satisfies (25). On the region $\tau \in (0, \infty)$, $x \in (x_f(\tau), \infty)$, both (2) and (25) have the same forms. □

Now we discuss the Laplace transform. For any complex value z with $\text{Re}(z) > 0$, the Laplace transform of $\mathbf{1}_{\{x \le x_f(\tau)\}}$:

$$\begin{aligned}\mathcal{L}[\mathbf{1}_{\{x \le x_f(\tau)\}}] &= \int_0^{+\infty} e^{-z\tau}\mathbf{1}_{\{x \le x_f(\tau)\}} d\tau = \int_0^{+\infty} e^{-z\tau}\mathbf{1}_{\{\tau \le \tau_f(x)\}} d\tau \\ &= \int_0^{\tau_f(x)} e^{-z\tau} d\tau = -\frac{1}{z} e^{-z\tau}\Big|_0^{\tau_f(x)} = \frac{1}{z}\left(1 - e^{-z\tau_f(x)}\right),\end{aligned} \tag{26}$$

where $\tau_f(x)$ is the inverse function of $x_f(\tau)$. Denote $\widehat{V}(x, z) = \mathcal{L}[V(x, \tau)](z)$. Then taking Laplace transform to the both sides of (25), we have

$$z\widehat{V}(x, z) - \nu_{-\infty} D_x^\alpha \widehat{V}(x, z) - (r - \nu)\frac{\partial \widehat{V}}{\partial x}(x, z) + r\widehat{V}(x, z) = \widehat{b}(x, z), \tag{27}$$

for all $x \in (\underline{x}, \infty)$, where

$$\widehat{b}(x, z) = (K - e^x)^+ + \frac{rK}{z}\left(1 - e^{-z\tau_f(x)}\right). \tag{28}$$

Taking Laplace transform to the boundary conditions (4), (5) and (6) and noting $e^x < K$ for $x < \underline{x}$ we get

$$\widehat{V}(x, z) = \frac{1}{z}\left(K - e^x\right), \quad x \le \underline{x}, \tag{29}$$

$$\frac{\partial \widehat{V}(x, z)}{\partial x} = -\frac{1}{z}e^x, \quad x \le \underline{x}, \tag{30}$$

$$\lim_{x \to +\infty} \widehat{V}(x, z) = 0. \tag{31}$$

Assume $x_L \ll \underline{x}$ such that ${}_{-\infty}D_x^{\alpha}\widehat{V}(x,z) \approx {}_{x_L}D_x^{\alpha}\widehat{V}(x,z)$ and x_R is sufficiently large such that $\widehat{V}(x_R,z) \approx 0$. Define

$$\Delta x = (x_R - x_L)/(N+1), \tag{32}$$

$$x_i = x_L + i\Delta x,\ i = 0, 1, \ldots, N+1. \tag{33}$$

Assume $\underline{x} = x_p$ for a certain $1 \le p \le N$, which can be easily done by selecting appropriate x_L and x_R. Denote $\widehat{V}_i(z) \approx \widehat{V}(x_i,z)$, $\widehat{b}_i(z) = \widehat{b}(x_i,z)$ for $i = p+1, p+2, \ldots, N$, and

$$\widehat{c}_i := -\frac{1}{\Delta x^{\alpha}} \sum_{k=i+1-p}^{i+1} g_k^{(\alpha)} \frac{K - e^{x_{i+1-k}}}{z}, \quad i = p+1, p+2, \ldots, N, \tag{34}$$

$$\widehat{\mathbf{c}} := [\widehat{c}_{p+1}, \widehat{c}_{p+2}, \ldots, \widehat{c}_N]^{\mathsf{T}}, \tag{35}$$

and

$$\begin{aligned} \widehat{\mathbf{v}}(z) &:= [\widehat{V}_{p+1}(z), \widehat{V}_{p+2}(z), \ldots, \widehat{V}_N(z)]^{\mathsf{T}}, \\ \widehat{\mathbf{b}}(z) &:= [\widehat{b}_{p+1}(z), \widehat{b}_{p+2}(z), \ldots, \widehat{b}_N(z)]^{\mathsf{T}}, \\ \widehat{\mathbf{f}}(z) &:= \widehat{\mathbf{b}}(z) - \widehat{\mathbf{c}}. \end{aligned} \tag{36}$$

Noting that $\widehat{V}_{N+1} = \widehat{V}(x_R,z) = 0$ and $\widehat{V}_k(z) = \frac{1}{z}(K - e^{x_k})$ for $k = p, p-1, \ldots, 0$, the finite difference method for the stationary fractional differential equation (27) can be expressed in a matrix form

$$(z\mathbf{I} - \mathbf{A})\widehat{\mathbf{v}}(z) = \widehat{\mathbf{f}}(z), \tag{37}$$

with

$$\mathbf{A} = \frac{\nu}{(\Delta x)^{\alpha}} \left(\mathbf{G}_{\alpha} + \frac{(\Delta x)^{\alpha}}{\nu} \mathbf{D} \right) \tag{38}$$

and

$$\mathbf{G}_{\alpha} = \begin{bmatrix} g_1^{(\alpha)} & g_0^{(\alpha)} & & & \\ g_2^{(\alpha)} & g_1^{(\alpha)} & g_0^{(\alpha)} & & \\ \vdots & \ddots & \ddots & \ddots & \\ g_{N-p-1}^{(\alpha)} & \cdots & g_2^{(\alpha)} & g_1^{(\alpha)} & g_0^{(\alpha)} \\ g_{N-p}^{(\alpha)} & \cdots & g_3^{(\alpha)} & g_2^{(\alpha)} & g_1^{(\alpha)} \end{bmatrix}, \tag{39}$$

$$\mathbf{D} = \begin{bmatrix} -r & \frac{\nu - r}{2\Delta x} & & & \\ -\frac{\nu - r}{2\Delta x} & -r & \frac{\nu - r}{2\Delta x} & & \\ & \ddots & \ddots & \ddots & \\ & & -\frac{\nu - r}{2\Delta x} & -r & \frac{\nu - r}{2\Delta x} \\ & & & -\frac{\nu - r}{2\Delta x} & -r \end{bmatrix}. \tag{40}$$

Noting that both $\mathbf{G}_{\alpha}$ and $\mathbf{A}$ are Toeplitz matrix [6], whose entries are constant along its diagonals. The Toeplitz structure is very important for the analysis of Laplace inversion in next section.

The result system (37) cannot be solved since an unknown function $\tau_f(x)$ is involved in it. Now, we give an approximation form of $\tau_f(x)$. As discussed in Sect. 2, $\tau_f(x)$ is a strictly

decreasing function on $[\underline{x}, \overline{x}]$ and $\tau_f(\overline{x}) = 0,\ \tau_f(\underline{x}) = +\infty$. So an approximation is given by

$$\tau_f(x) \approx \tau_f(x;\gamma,\beta) = \begin{cases} 0, & x \geq \overline{x}, \\ \gamma\left(-\log\frac{x-\underline{x}}{\overline{x}-\underline{x}}\right)^{\beta}, & \underline{x} < x < \overline{x}, \\ +\infty, & x = \underline{x}, \end{cases} \tag{41}$$

where $\gamma \geq 0$ and $\beta \geq 1$ (Noting that $\beta \geq 1$ ensures that $\tau_f(x)$ is a convex function) are two constant numbers to be determined by optimization (45) (see below). Denote $\mathbf{a}(z)$ be the first row of $(z\mathbf{I} - \mathbf{A})^{-1}$. Then $\mathbf{a}(z)$ can be obtained by solving linear system:

$$\mathbf{a}(z)(z\mathbf{I} - \mathbf{A}) = [1, 0, 0, \ldots, 0]. \tag{42}$$

Therefore, the first component in the solution vector $\widehat{\mathbf{v}}(z)$ has the following expression

$$\widehat{V}_{p+1}(z) = \mathbf{a}(z)\widehat{\mathbf{f}}(z;\gamma,\beta), \tag{43}$$

where $\widehat{\mathbf{f}}(z;\gamma,\beta) = \widehat{\mathbf{f}}(z)$ defined in (36), in which it involves (41), the approximation of $\tau_f(x_i),\ i = p+1, p+2, \ldots, N$. We find the parameters $\gamma,\ \beta$ such that condition (30) holds for all real values of $z > 0$. A practicable way is to consider a sequence of $z_1, z_2, \ldots, z_m$ ($m \geq 2$) and find the values of unknown $\gamma,\ \beta$ that minimize the sum of residue,

$$\min_{\gamma\geq 0,\,\beta\geq 1} \sum_{k=1}^{m} \left[\frac{\widehat{V}_{p+1}(z_k) - \widehat{V}_{p-1}(z_k)}{2\Delta x} - \frac{\partial \widehat{V}(x, z_k)}{\partial x}\Big|_{x=x_p} \right]^2, \tag{44}$$

which becomes, by inserting (30), (43) and $\widehat{V}_{p-1}(z_k) = \frac{1}{z_k}(K - e^{x_{p-1}})$ into (44), that

$$\min_{\gamma\geq 0,\,\beta\geq 1} \sum_{k=1}^{m} \left[\frac{\mathbf{a}(z_k)\widehat{\mathbf{f}}(z_k;\gamma,\beta) - \frac{1}{z_k}(K - e^{x_{p-1}})}{2\Delta x} + \frac{e^{x_p}}{z_k} \right]^2. \tag{45}$$

After solving the optimal exercise boundary $x_f(\tau) = \tau_f^{-1}(x)$, we can solve the linear system (37) to get the values $\widehat{V}_i$ for $i = p+1, p+2, \ldots, N$. Then, we use numerical Laplace inversion to compute the American option valves

$$V(x_i, \tau) = \mathcal{L}^{-1}[\widehat{V}_i(z)], \quad i = p+1, p+2, \ldots, N. \tag{46}$$

The detailed computational procedure is summarized in Algorithm 3.

Algorithm 3 Laplace transform method for solving (2)

Step 1. Apply Algorithm 2 to compute $\underline{x}$;
Step 2. Optimize (45) to get $\tau_f(x)$;
Step 3. Compute $\widehat{\mathbf{V}}(z)$ by solving Eq. (37);
Step 4. Apply Laplace inversion to restore American values $V(x_i, \tau)$.

Apparently the Laplace inversion plays a key role in the Laplace transform method—Algorithm 3. In next section, we propose a fast Laplace inversion based on hyperbolic contour integral method.

4 Hyperbolic Contour Integral Method for Laplace Inversion

The inversion of Laplace transform is based on numerical integration of the Bromwich complex contour integral

$$V(x,\tau)=\frac{1}{2\pi\imath}\int_{\eta-\imath\infty}^{\eta+\imath\infty}e^{z\tau}\widehat{V}(x,z)\mathrm{d}z,\quad \eta>\eta_0, \tag{47}$$

where $\imath=\sqrt{-1}$ and η_0 is the convergence abscissa. This means that all the singularities of $\widehat{V}(x,z)$ (with respect to z) lie in the open half-plane $\mathrm{Re}(z)\le\eta_0$. The integral (47) is not well-suited for numerical integration. First, the exponential factor is highly oscillatory on the Bromwich line, $z=\eta+\imath y, -\infty<y<+\infty$. Second, the transform $\widehat{V}(x,z)$ typically decays slowly as $|y|\to\infty$. One strategy for circumventing the slow decay is due to Talbot [32], who suggests that the Bromwich line be deformed into a contour Γ that begins and ends in the left half-plane, such that $\mathrm{Re}(z)\to-\infty$ at each end. On such a contour, the exponential factor in (47) forces a rapid decay of the integrand as $\mathrm{Re}(z)\to-\infty$. This makes the integral well suited for approximation by the trapezoidal or midpoint rules. Owing to Cauchys theorem, such a deformation of contour is permissible as long as no singularities are traversed in the process, and provided that $\widehat{V}(x,z)\to 0$ uniformly in $\mathrm{Re}(z)\le\eta_0$ as $|z|\to\infty$.

Denote

$$\mathbf{x}=[x_{p+1},x_{p+2},\ldots,x_N]^{\mathsf{T}}, \tag{48}$$

$$\mathbf{v}(\tau)\triangleq\mathbf{v}(\mathbf{x},\tau)=[V(x_{p+1},\tau),V(x_{p+2},\tau),\ldots,V(x_N,\tau)]^{\mathsf{T}}. \tag{49}$$

The Laplace inversion of $\widehat{\mathbf{v}}(z)=(z\mathbf{I}-\mathbf{A})^{-1}\widehat{\mathbf{f}}(z)$ with respect to z can be expressed as

$$\begin{aligned}\mathbf{v}(\tau)&=\frac{1}{2\pi\imath}\int_\Gamma e^{z\tau}\widehat{\mathbf{v}}(z)\mathrm{d}z\\&=\frac{1}{2\pi\imath}\int_\Gamma e^{z\tau}(z\mathbf{I}-\mathbf{A})^{-1}\widehat{\mathbf{f}}(z)\mathrm{d}z\\&=\frac{1}{2\pi\imath}\int_\Gamma e^{z\tau}(z\mathbf{I}-\mathbf{A})^{-1}(\widehat{\mathbf{b}}(z)-\widehat{\mathbf{c}})\mathrm{d}z.\end{aligned} \tag{50}$$

This is the vector version of Laplace inversion (47). Unfortunately, the idea of Talbot cannot be applied directly, since $|\widehat{\mathbf{f}}(z)|\to\mathbf{0}$ (as $|z|\to\infty$) is not true. If we split

$$\widehat{\mathbf{f}}(z)=\widehat{\mathbf{b}}(z)-\widehat{\mathbf{c}}=\widehat{\mathbf{f}}_1(z)+\widehat{\mathbf{f}}_2(z), \tag{51}$$

with

$$\begin{cases}\widehat{\mathbf{f}}_1(z)=[\widehat{f}_{1,p+1}(z),\widehat{f}_{1,p+2}(z),\ldots,\widehat{f}_{1,N}(z)]^{\mathsf{T}},\\ \widehat{\mathbf{f}}_2(z)=[\widehat{f}_{2,p+1}(z),\widehat{f}_{2,p+2}(z),\ldots,\widehat{f}_{2,N}(z)]^{\mathsf{T}},\end{cases} \tag{52}$$

where

$$\widehat{f}_{1,j}(z)=(K-e^{x_j})^+ +\frac{rK}{z}-\widehat{c}_j-\frac{rK}{z}e^{-z\tau_f(x_j)}\mathbf{1}_{\{\tau-\tau_f(x_j)>0\}}, \tag{53}$$

and

$$\widehat{f}_{2,j}(z)=-\frac{rK}{z}e^{-z\tau_f(x_j)}\mathbf{1}_{\{\tau-\tau_f(x_j)\le 0\}} \tag{54}$$

for $j=p+1,p+2,\ldots,N$. The expressions (53) and (54) come from the decompose of $\widehat{b}(x,z)$ (see expression (28)). Then $e^{z\tau}|\widehat{\mathbf{f}}_1(z)|\to\mathbf{0}$ as $\mathrm{Re}(z)\to-\infty$ and $e^{z\tau}|\widehat{\mathbf{f}}_2(z)|\to\mathbf{0}$ as $\mathrm{Re}(z)\to+\infty$.

Denoting $\widehat{\mathbf{v}}_k(z) = (z\mathbf{I} - \mathbf{A})^{-1}\widehat{\mathbf{f}}_k(z)$ $(k = 1, 2)$ and using (51)–(54), we re-define the Laplace inversion as

$$\begin{aligned}\mathbf{v}(\tau) &= \mathbf{v}_1(\tau) + \mathbf{v}_2(\tau)\\ &= \frac{1}{2\pi\imath}\int_{\Gamma_1} e^{z\tau}\widehat{\mathbf{v}}_1(z)\mathrm{d}z + \frac{1}{2\pi\imath}\int_{\Gamma_2} e^{z\tau}\widehat{\mathbf{v}}_2(z)\mathrm{d}z\\ &= \frac{1}{2\pi\imath}\int_{\Gamma_1} e^{z\tau}(z\mathbf{I} - \mathbf{A})^{-1}\widehat{\mathbf{f}}_1(z)\mathrm{d}z + \frac{1}{2\pi\imath}\int_{\Gamma_2} e^{z\tau}(z\mathbf{I} - \mathbf{A})^{-1}\widehat{\mathbf{f}}_2(z)\mathrm{d}z. \end{aligned} \tag{55}$$

In next paragraphs, we will prove that the spectrum $\Lambda(\mathbf{A})$ lies in a sectorial region Σ_δ which locates in the left half-plane. It is necessary to analyze the properties of $\widehat{\mathbf{f}}_1(z)$ and $\widehat{\mathbf{f}}_2(z)$. Observing (52) and (55), we find $e^{z\tau}\widehat{\mathbf{v}}_1(z) \to \mathbf{0}$ as $\mathrm{Re}(z) \to -\infty$ whereas $e^{z\tau}\widehat{\mathbf{v}}_2(z) \to \mathbf{0}$ as $\mathrm{Re}(z) \to +\infty$. In practical computations, the curve Γ_1 in $\mathbf{v}_1(\tau)$ is often deformed to a special Hankel contour whose real part begins at the negative infinity in the third quadrant, then winds anticlockwise around all singularities of $\widehat{\mathbf{v}}_1(z)$ and last terminates with the real part again going to infinity in the second quadrant. Similarly, the real part of the curve Γ_2 in $\mathbf{v}_2(\tau)$ should begin at the positive infinity in the fourth quadrant, then winds clockwise around all singularities of $\widehat{\mathbf{v}}_2(z)$ and last terminates with the real part again going to infinity in the first quadrant.

Based on the analysis of Weideman [35] (see also Pang and Sun [24]), we select the hyperbolic contour Γ_1, which can be parameterized by

$$\Gamma_1 : z(\zeta) = \mu[1 + \sin(\imath\zeta - \theta)], \quad -\infty < \zeta < \infty, \tag{56}$$

where parameters $\mu > 0$ and θ set the width and the asymptotic angle of the hyperbolic contour, respectively. Then substituting the contour (56) into (55) gives

$$\mathbf{v}_1(\tau) = \frac{1}{2\pi\imath}\int_{\Gamma_1} e^{z\tau}\widehat{\mathbf{v}}_1(z)\mathrm{d}z = \frac{1}{2\pi\imath}\int_{-\infty}^{+\infty} e^{z(\zeta)\tau}z'(\zeta)\widehat{\mathbf{v}}_1(z(\zeta))\mathrm{d}\zeta. \tag{57}$$

Discretization of this integral with uniform node spacing h yields

$$\begin{aligned}\mathbf{v}_1(\tau) &= \frac{h}{2\pi\imath}\sum_{k=-\infty}^{+\infty} e^{z(\zeta_k)\tau}z'(\zeta_k)\widehat{\mathbf{v}}_1(z(\zeta_k)) + DE_+(h) + DE_-(h)\\ &= \frac{h}{2\pi\imath}\sum_{k=-L}^{L} e^{z(\zeta_k)\tau}z'(\zeta_k)\widehat{\mathbf{v}}_1(z(\zeta_k)) + DE_+(h) + DE_-(h) + TE(hL), \end{aligned} \tag{58}$$

where $\zeta_k = kh$ for the trapezoidal rule and $\zeta_k = (k + \frac{1}{2})h$ for the midpoint rule, L is the number of quadrature nodes, $DE_\pm(h)$ are the discretization errors and $TE(hL)$ is the truncation error. Define

$$g_\tau(\zeta) = \frac{1}{2\pi\imath}e^{z(\zeta)\tau}z'(\zeta)\widehat{\mathbf{v}}_1(z(\zeta)),$$

and assume the function $g_\tau(\zeta + \imath d)$ be analytic in the strip $d \in (d_-, d_+)$ with $d_+ > 0$ and $d_- < 0$. Then the discretization errors are bounded as

$$\|DE_+(h)\| = \frac{M(d_+)}{e^{2\pi d_+/h} - 1}, \quad \|DE_-(h)\| = \frac{M(d_-)}{e^{-2\pi d_-/h} - 1},$$

where

$$M(d) = \int_{-\infty}^{+\infty} \|g_\tau(\zeta + \imath d)\|d\zeta, \quad d = d_+ \,(\text{or}\, d_-)$$

and $\|\cdot\|$ is some vector norm. The truncation error $TE(hL)$ can be approximated by the magnitude of the last term retained, i.e.,

$$\|TE(hL)\| = \mathcal{O}(\|g_\tau(hL)\|), \quad L \to \infty.$$

To make all the singularities of the integrand in (57) to fall into a sectorial region

$$\Sigma_\delta = \left\{ z \in \mathbb{C} : \ |\arg(-z)| \le \delta, \ \delta \in \left(0, \frac{\pi}{2}\right) \right\}. \tag{59}$$

By asymptotically matching $\|DE_\pm(h)\|$ to $\|TE(hL)\|$, h and μ are derived as follows:

$$h = \frac{\rho(\theta)}{L}, \quad \mu = \frac{4\pi\theta - \pi^2 + 2\pi\delta}{\rho(\theta)} \frac{L}{\tau}, \quad \rho(\theta) = \cosh^{-1}\left(\frac{2\theta}{(4\theta - \pi + 2\delta)\sin\theta} \right) \tag{60}$$

and θ is a free parameter. With the choice the predicted convergence rate is given by

$$\left\| \mathbf{v}_1(\tau) - \frac{h}{2\pi\imath} \sum_{k=-L}^{L} e^{z(\zeta_k)\tau} z'(\zeta_k) \widehat{\mathbf{v}}_1(z(\zeta_k)) \right\| \le \mathcal{O}\left(e^{-R(\theta)L} \right), \tag{61}$$

where

$$R(\theta) = \frac{\pi^2 - 2\pi\theta - 2\pi\delta}{\rho(\theta)}, \tag{62}$$

and $\|\cdot\|$ is some vector norm. The analysis of (58)–(62) can be found in [34,35] or [24]. According to (61), we see that once the semi-angle δ of the sectorial region (59) is given, then one can find the optimal θ by maximizing the function $R(\theta)$. Consequently, the optimal parameters h and μ can be obtained from the formulas (60).

The curve Γ_2 can be selected as the right-hand branch of hyperbola

$$\Gamma_2 : \ z(\zeta) = \mu[1 + \sin(\imath\zeta + \theta)], \quad -\infty < \zeta < \infty, \tag{63}$$

where parameters h and μ are given by formulas (60) with setting $\delta = 0$, and

$$\mathbf{v}_2(\tau) \approx \frac{h}{2\pi\imath} \sum_{k=-L}^{L} e^{z(\zeta_k)\tau} z'(\zeta_k) \widehat{\mathbf{v}}_2(z(\zeta_k)). \tag{64}$$

The shapes and location of hyperbolas Γ_1 and Γ_2 are plotted in Fig. 2.

In following paragraphs, we prove all singularities of the Toeplitz matrix $\mathbf{A}$ defined by (38) fall into a sectorial region Σ_δ. To this end, we introduce some properties of Toeplitz matrix. A matrix that has the following form

$$\mathbb{A} = \begin{bmatrix} a_0 & a_{-1} & \cdots & a_{2-n} & a_{1-n} \\ a_1 & a_0 & a_{-1} & \cdots & a_{2-n} \\ \vdots & a_1 & a_0 & \ddots & \vdots \\ a_{n-2} & \cdots & \ddots & \ddots & a_{-1} \\ a_{n-1} & a_{n-2} & \cdots & a_1 & a_0 \end{bmatrix}, \tag{65}$$

is called a Toeplitz matrix [6], whose entries are constant along its diagonals. If the diagonals of matrix $\mathbb{A}$ are the Fourier coefficients of a function f, i.e.,

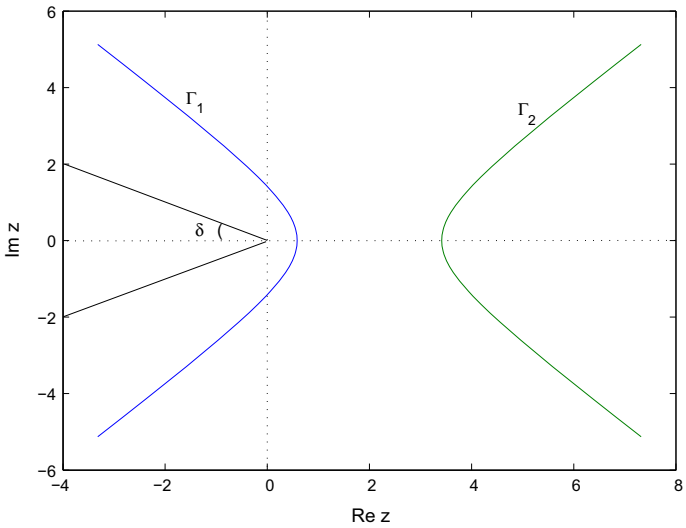

Fig. 2 The hyperbolic contour Γ_1 and Γ_2 with $\mu = 2, \theta = \pi/4$. Γ_1 encloses the sectorial region Σ_δ with $\delta = \arctan \frac{1}{2}$

$$a_k = \frac{1}{2\pi} \int_{-\pi}^{\pi} f(\eta) e^{-\iota k \eta} \mathrm{d}\eta \tag{66}$$

then the function f is called the generating function of $\mathbb{A}$.

Let $\mathbb{A} \in \mathbb{C}^{n\times n}$ be a square matrix. The numerical range of $\mathbb{A}$ is defined as

$$\mathcal{W}(\mathbb{A}) = \{\mathbf{v}^* \mathbb{A} \mathbf{v} : \mathbf{v} \in \mathbb{C}^{n\times n}, \mathbf{v}^* \mathbf{v} = 1\}, \tag{67}$$

and the angular numerical range of $\mathbb{A}$ is defined as

$$\mathcal{W}'(\mathbb{A}) = \{\mathbf{v}^* \mathbb{A} \mathbf{v} : \mathbf{v} \in \mathbb{C}^{n\times n}\}. \tag{68}$$

It is clear that $\mathcal{W}'(\mathbb{A})$ is a sectorial region of the complex plane that is anchored at the origin. The field angle is just the angular opening of the smallest angular sector that includes $\mathcal{W}(\mathbb{A})$ (see e.g., [10]).

Let

$$\Omega(f) := \{f(\eta) | \eta \in (-\pi, \pi)\}$$

denote the range of f, and $\mathrm{conv}(\Omega(f))$ the convex hull of $\Omega(f)$. Lemmas 1 and 2 reveal the relationship between the numerical range $\mathcal{W}(\mathbb{A})$, spectrum $\Lambda(\mathbb{A})$ and the generating function $f(\eta)$ of a Toeplitz matrix $\mathbb{A}$.

Lemma 1 (see [16,33]) *Suppose that the function $f(\eta)$ for $\eta \in (-\pi, \pi)$ is continuous. Let $\mathbb{A} \in \mathbb{C}^{n\times n}$ be a Toeplitz matrix generated by $f(\eta)$. Then $\mathcal{W}(\mathbb{A})$ is a subset of the closure of* $\mathrm{conv}(\Omega(f))$, *i.e.,*

$$\mathcal{W}(\mathbb{A}) \subseteq \overline{\mathrm{conv}(\Omega(f))}. \tag{69}$$

Lemma 2 (see [24]) *Let $\mathbb{A}$, $\mathbb{D} \in \mathbb{C}^{n\times n}$. Suppose that $\mathbb{D}$ is positive definite. Then*

$$\Lambda(\mathbb{D}\mathbb{A}) \subseteq \mathcal{W}'(\mathbb{A}). \tag{70}$$

Theorem 2 *Let* $\widetilde{\mathbf{A}} = \mathbf{G}_\alpha + \frac{(\Delta x)^\alpha}{\nu}\mathbf{D}$ *with* $\mathbf{G}_\alpha$ *and* $\mathbf{D}$ *being given by* (39) *and* (40)*, respectively. Then the generating function of* $\widetilde{\mathbf{A}}$ *is given by*

$$f(\eta) = \begin{cases} \left(2\sin\frac{\eta}{2}\right)^\alpha \left[\cos\left(\frac{\alpha\pi}{2} + \left(1-\frac{\alpha}{2}\right)\eta\right) - \iota\sin\left(\frac{\alpha\pi}{2} + \left(1-\frac{\alpha}{2}\right)\eta\right)\right] \\ -\frac{r(\Delta x)^\alpha}{\nu} - \iota\frac{(\nu-r)(\Delta x)^{\alpha-1}}{\nu}\sin\eta, \qquad \eta\in(0,\pi), \\ \left(-2\sin\frac{\eta}{2}\right)^\alpha \left[\cos\left(\frac{\alpha\pi}{2} + \left(\frac{\alpha}{2}-1\right)\eta\right) + \iota\sin\left(\frac{\alpha\pi}{2} + \left(\frac{\alpha}{2}-1\right)\eta\right)\right] \\ -\frac{r(\Delta x)^\alpha}{\nu} - \iota\frac{(\nu-r)(\Delta x)^{\alpha-1}}{\nu}\sin\eta, \qquad \eta\in(-\pi,0). \end{cases} \tag{71}$$

Proof According to (39) and (40), the generating function f of $\widetilde{\mathbf{A}}$ can be written as

$$\begin{aligned} f(\eta) &= \sum_{k=0}^{\infty} g_k^{(\alpha)} e^{\iota(k-1)\eta} - \frac{r(\Delta x)^\alpha}{\nu} - \frac{(\nu-r)(\Delta x)^\alpha}{2\nu\Delta x}e^{\iota\eta} + \frac{(\nu-r)(\Delta x)^\alpha}{2\nu\Delta x}e^{-\iota\eta} \\ &= e^{-\iota\eta}\sum_{k=0}^{\infty} g_k^{(\alpha)} e^{\iota k\eta} - \frac{r(\Delta x)^\alpha}{\nu} - \iota\frac{(\nu-r)(\Delta x)^{\alpha-1}}{\nu}\sin\eta. \end{aligned} \tag{72}$$

Noting that $g_k^{(\alpha)}$ in fact are the coefficients of the power series of the function $(1-z)^\alpha$, i.e.,

$$(1-z)^\alpha = \sum_{k=0}^{\infty} g_k^{(\alpha)} z^k, \quad |z| \le 1, \tag{73}$$

we have

$$\begin{aligned} f(\eta) &= e^{-\iota\eta}(1-e^{\iota\eta})^\alpha - \frac{r(\Delta x)^\alpha}{\nu} - \iota\frac{(\nu-r)(\Delta x)^{\alpha-1}}{\nu}\sin\eta \\ &= e^{-\iota\eta}\left(2\iota\sin\left(-\frac{\eta}{2}\right)e^{\iota\frac{\eta}{2}}\right)^\alpha - \frac{r(\Delta x)^\alpha}{\nu} - \iota\frac{(\nu-r)(\Delta x)^{\alpha-1}}{\nu}\sin\eta, \end{aligned} \tag{74}$$

from which the expression of (71) can be obtained. □

Using Young's inequality, we can prove that both the numerical range and angular numerical range of $\widetilde{\mathbf{A}}$ fall in a sectorial region Σ_δ.

Theorem 3 *Let* $\widetilde{\mathbf{A}} \equiv \mathbf{G}_\alpha + \frac{(\Delta x)^\alpha}{\nu}\mathbf{D}$ *with* $\mathbf{G}_\alpha$ *and* $\mathbf{D}$ *being given by* (39) *and* (40)*, respectively. Then the numerical range* $\mathcal{W}(\widetilde{\mathbf{A}})$ *of* $\widetilde{\mathbf{A}}$ *lies in a sectorial region* Σ_δ *such that*

$$\mathcal{W}(\widetilde{\mathbf{A}}) \subseteq \Sigma_\delta \equiv \{z\in\mathbb{C} : |\arg(-z)| \le \delta\}, \tag{75}$$

with

$$\delta = \arctan\left(\left|\tan\left(\frac{\alpha\pi}{2}\right)\right| + |\nu - r|r^{\frac{1-\alpha}{\alpha}}\nu^{-\frac{1}{\alpha}}\left(-\alpha\cos\frac{\alpha\pi}{2}\right)^{-\frac{1}{\alpha}}\left(\frac{\alpha}{\alpha-1}\right)^{\frac{1-\alpha}{\alpha}}\right). \tag{76}$$

Furthermore,

$$\mathcal{W}'(\widetilde{\mathbf{A}}) \subseteq \Sigma_\delta. \tag{77}$$

Proof From (71) and noting $\left(\frac{\alpha\pi}{2} + \left(\frac{\alpha}{2}-1\right)\eta\right) \in (\frac{\alpha\pi}{2}, \pi)$, it is easy to show that the real part of $f(\eta)$,

$$\mathrm{Re}(f(\eta)) = \left|2\sin\frac{\eta}{2}\right|^\alpha \cos\left(\frac{\alpha\pi}{2} + \left(\frac{\alpha}{2}-1\right)\eta\right) - \frac{r\Delta x^\alpha}{\nu} < -\frac{r\Delta x^\alpha}{\nu}$$

for $\eta \in (-\pi, \pi),\ 1 < \alpha < 2$. Let $p = \alpha,\ q = \frac{\alpha}{\alpha-1}$. Then $\frac{1}{p} + \frac{1}{q} = 1$. Let

$$a = 2\left(\sin\frac{\eta}{2}\right)\left[-\alpha\cos\left(\frac{\alpha\pi}{2} + \left(1-\frac{\alpha}{2}\right)\eta\right)\right]^{\frac{1}{\alpha}}, \tag{78}$$

$$b = \left(\frac{r\alpha}{\nu(\alpha-1)}\right)^{\frac{\alpha-1}{\alpha}} (\Delta x)^{\alpha-1}. \tag{79}$$

Then using Young's inequality we have

$$\begin{aligned}|\mathrm{Re}(f(\eta))| &= \frac{a^p}{p} + \frac{b^q}{q} \geq ab \\ &= 2\left(\sin\frac{\eta}{2}\right)\left[-\alpha\cos\left(\frac{\alpha\pi}{2} + \left(1-\frac{\alpha}{2}\right)\eta\right)\right]^{\frac{1}{\alpha}} \left(\frac{r\alpha}{\nu(\alpha-1)}\right)^{\frac{\alpha-1}{\alpha}} (\Delta x)^{\alpha-1}.\end{aligned}$$

Therefore,

$$\begin{aligned}\left|\frac{\mathrm{Im}(f(\eta))}{\mathrm{Re}(f(\eta))}\right| &\leq \frac{\left(2\sin\frac{\eta}{2}\right)^{\alpha}\left|\sin\left(\frac{\alpha\pi}{2} + \left(1-\frac{\alpha}{2}\right)\eta\right)\right|}{\left(2\sin\frac{\eta}{2}\right)^{\alpha}\left|\cos\left(\frac{\alpha\pi}{2} + \left(1-\frac{\alpha}{2}\right)\eta\right)\right|} + \frac{\left|\frac{(\nu-r)(\Delta x)^{\alpha-1}}{\nu}\sin\eta\right|}{|\mathrm{Re}(f(\eta))|} \\ &\leq \left|\tan\left(\frac{\alpha\pi}{2}\right)\right| + \frac{|2\sin\frac{\eta}{2}\cos\frac{\eta}{2}||\nu-r|(\Delta x)^{\alpha-1}}{\nu ab} \\ &= \left|\tan\left(\frac{\alpha\pi}{2}\right)\right| + \frac{|\nu-r|}{\left[-\alpha\cos\left(\frac{\alpha\pi}{2} + \left(1-\frac{\alpha}{2}\right)\eta\right)\right]^{\frac{1}{\alpha}} r^{\frac{\alpha-1}{\alpha}} \nu^{\frac{1}{\alpha}}} \\ &\leq \left|\tan\left(\frac{\alpha\pi}{2}\right)\right| + \frac{|\nu-r|}{\left[-\alpha\cos\left(\frac{\alpha\pi}{2}\right)\right]^{\frac{1}{\alpha}} r^{\frac{\alpha-1}{\alpha}} \nu^{\frac{1}{\alpha}}} \\ &\leq \left|\tan\left(\frac{\alpha\pi}{2}\right)\right| + |\nu-r| r^{\frac{1-\alpha}{\alpha}} \nu^{-\frac{1}{\alpha}} \left|\alpha\cos\frac{\alpha\pi}{2}\right|^{-\frac{1}{\alpha}} \left(\frac{\alpha}{\alpha-1}\right)^{\frac{1-\alpha}{\alpha}},\end{aligned}$$

which shows that $\Omega(f(\eta)) \subseteq \Sigma_\delta$. Apparently the sectorial region Σ_δ is a closed convex hull. Therefore, From Lemma 1 we have

$$\mathcal{W}(\widetilde{\mathbf{A}}) \subseteq \overline{\mathrm{conv}(\Omega(f))} \subseteq \Sigma_\delta.$$

Recall that $\mathcal{W}'(\widetilde{\mathbf{A}})$ is also a sectorial region whose angle is just the angular opening of the smallest angular sector that includes$\mathcal{W}(\widetilde{\mathbf{A}})$. Therefore we have

$$\mathcal{W}'(\widetilde{\mathbf{A}}) \subseteq \Sigma_\delta,$$

which ends the proof. □

With the help of the generating function of $\widetilde{\mathbf{A}}$, we can further prove that the spectrum of the matrix $\mathbf{A} \equiv \frac{\nu}{(\Delta x)^\alpha}\widetilde{\mathbf{A}}$, which is just the discrete matrix of the Laplace transform method (see (38)), is contained in a sectorial region Σ_δ (see Fig. 2.). This guarantees that the inversion formulas (58) and (64) can be properly used.

Theorem 4 *Let* $\mathbf{A} \equiv \frac{\nu}{(\Delta x)^\alpha}\widetilde{\mathbf{A}} = \frac{\nu}{(\Delta x)^\alpha}\left(\mathbf{G}_\alpha + \frac{(\Delta x)^\alpha}{\nu}\mathbf{D}\right)$ *with* $\mathbf{G}_\alpha$ *and* $\mathbf{D}$ *being given by* (39) *and* (40)*, respectively. Then the spectrum* $\Lambda(\mathbf{A})$ *of the resulting coefficient matrix* $\mathbf{A}$ *given by* (38) *lies in the sectorial region* Σ_δ *defined by* (75) *and* (76)*, i.e.,*

$$\Lambda(\mathbf{A}) \subseteq \Sigma_\delta. \tag{80}$$

Furthermore, we have

$$\|(z\mathbf{I}-\mathbf{A})^{-1}\| \le \frac{1}{\mathrm{dist}(z,\,\Sigma_\delta)}, \quad z \notin \Sigma_\delta. \tag{81}$$

Proof From Lemma 2 we have

$$\Lambda(\mathbf{A}) = \Lambda\left(\frac{\nu}{(\Delta x)^\alpha}\widetilde{\mathbf{A}}\right) \subseteq \mathcal{W}'(\widetilde{\mathbf{A}})$$

and from Theorem 3 we have

$$\mathcal{W}'(\widetilde{\mathbf{A}}) \subseteq \Sigma_\delta.$$

Therefore

$$\Lambda(\mathbf{A}) \subseteq \mathcal{W}'(\widetilde{\mathbf{A}}) \subseteq \Sigma_\delta$$

and inequality (81) is proved. □

5 Numerical Examples

In this section, we illustrate the efficiency of the Laplace transform methods (LTMs) for American option pricing problem (2)–(6). The results of LTMs are compared with finite difference methods (FDMs). The values of the parameters are taken as $T = 2$ (year), $r = 0.05$ (1/year), $K = 40$ (dollar), $x_L = -40$ and $x_R = 10$. The space mesh partition number $N = 4999$ for LTMs and FDMs, the time meshsize $\Delta t = T/6000$ for FDM. The positive values $z_k = k$ $(k = 1, 2, \ldots, m)$ with $m = 4$ (see expression (45)). Also the performances of the Laplace inversion GS formula in [31] and hyperbolic contour integral (HCI) are compared. We take the parameter $L = 6$ in numerical Laplace inversion GS formula and hyperbolic contour integrals (58) and (64). The Matlab command "fminsearch" is used to search the approximate parameters γ and β with initial values $\gamma = 1,\ \beta = 1$. We use Matlab command "\" to get the vector $(z\mathbf{I}-\mathbf{A})^{-1}\mathbf{f}_k(z)$ for the LTM expression (55) for $k = 1, 2$ and $[\mathbf{A}^{(p)}]^{-1}\mathbf{b}^{(j,p)}$ for FDM expression (14).

In all tables and figures, the label "LTM" represents the LTM using (41) for approximation of $\tau_f(x)$, "LTM-GS" represents the LTM using GS Laplace inversion formula in [31], and "LTM-HCI" represents the LTM using the hyperbolic contour integrals (58) and (64).

All the numerical experiments are run in MATLAB 7.9.0 (R2009b) on a PC with the configuration: Intel(R) Core(TM) i5-4200 CPU @ 2.5GHz and 4.00GB RAM.

Example 1 In this example we compare the optimal exercise boundaries obtained by LTMs and FDMs with different volatility σ and diffusion order α. Figure 3 plots the free boundaries with $\sigma = 0.2,\ 0.3$ and $\alpha = 1.8,\ 1.9$. It can be seen from the figure that the optimal exercise boundaries obtained by the LTMs are very close to that by the FDMs.

Example 2 In this example, we compare the option values, relative errors and the computational time (CPU time) obtained by LTM-HCI, LTM-GS, and FDM with different volatility σ and diffusion order α. Table 1 lists the numerical results. The relative errors (RE-HCI and RE-GS) shown in the table are the absolute difference between the computed numerical values and the FDM benchmark divided by FDM benchmark. From this table we see that LTM-HCI is more accurate than the LTM-GS as the relative errors for LTM-HCI is much smaller than LTM-GS. Moreover the computational time for LTMs (LTM-HCI and LTM-GS) is much less than the FDM.

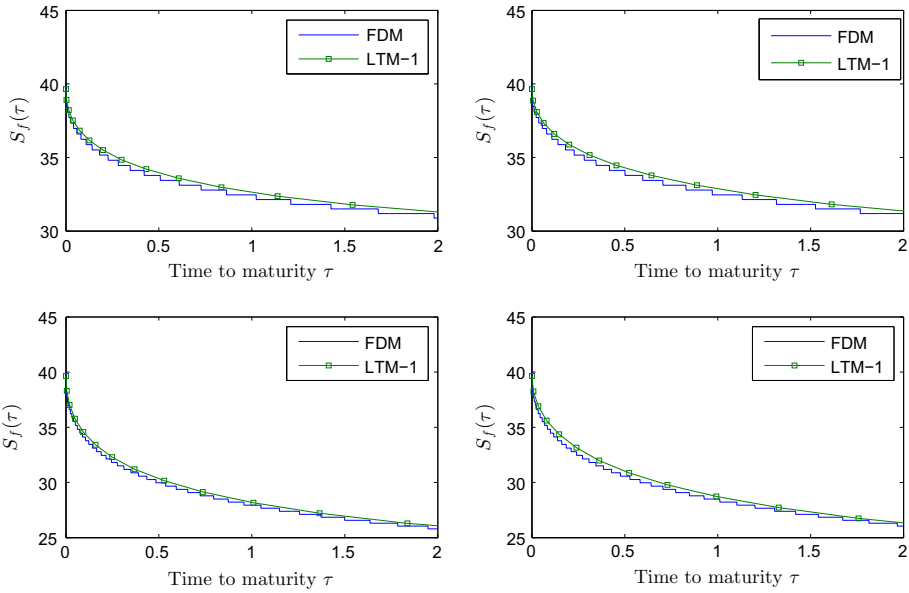

Fig. 3 Optimal exercise boundaries $S_f(\tau) = e^{x_f(\tau)}$ computed by FDMs and LTMs with different volatility σ and different diffusion order α. *Left-top* $\sigma = 0.2$, $\alpha = 1.9$; *right-top* $\sigma = 0.2$, $\alpha = 1.8$; *left-bottom* $\sigma = 0.3$, $\alpha = 1.9$; *right-bottom* $\sigma = 0.3$, $\alpha = 1.8$

Example 3 The convergence speed of the LTM-HCI method is controlled by the number of space mesh N and the parameter L for the numerical Laplace inversion. In this example, we illustrate the convergence rates of the LTM-HCI methods with N and L. In addition we examine the effect of the vanishing truncated boundary conditions by comparing the solutions with different truncated boundaries x_L and x_R.

To study the convergence rate with respect to N, we use Algorithm 2 to compute $\underline{x}$. Set the left and right boundary as

$$x_L = \underline{x} - 18(\overline{x} - \underline{x}), \quad x_R = \overline{x} + (\overline{x} - \underline{x}),$$

with $\overline{x} = \log K$. We compute the LTM-HCI numerical solutions with different number of space mesh as listed in Table 2. We take the parameter $L = 6$ in numerical Laplace inversion GS formula and hyperbolic contour integrals (58) and (64). Table 2 shows that the convergence rate of the LTM-HCI method with respect to N is about 1.

To investigate the convergence rate of the LTM-HCI method with respect to L, we compute the LTM-HCI solutions with the truncated boundaries $x_L = \overline{x} - 40$, $x_R = \overline{x} + 10$, number of space mesh $N = 6999$, and different values of L. We draw Fig. 4 for the errors where the vertical coordinate uses log-scale. In Fig. 4 the "solid line" represents the computational error and the "dot line" the theoretical error. We observe that the computational error roughly behaves proportional to the theoretical ones $\exp(-1.7680L)$, which means that the error exponentially decays.

We plot the solutions (option values) of the LTM-HCL method with different boundary truncation x_L and x_R in Fig. 5. From Fig. 5, we see that the LTM-HCI solution (solid line) obtained with $x_L = -40$, $x_R = 10$ is very close to the one (dot line) computed with $x_L = -80$, $x_R = 20$. This means that the vanishing truncated boundary condition does not have much effect to the accuracy of computation.

Table 1 Computational results (option values, relative errors and CPU time) with parameters $\tau = 2$, $r = 0.05$, $K = 40$, $N = 5000$, $M = 6000$, and different values of volatility σ and diffusion order α

S_0	LTM-HCI	RE-HCI (%)	LTM-GS	RE-GS (%)	FDM
$\sigma = 0.1,\ \alpha = 1.9$					
30	10.0000	0.000	10.0000	0.000	10.0000
35	5.0000	0.000	5.0000	0.000	5.0000
40	1.2847	0.221	1.2866	0.368	1.2819
45	0.3697	0.227	0.3719	0.814	0.3689
50	0.1519	0.120	0.1537	1.315	0.1518
$\sigma = 0.2,\ \alpha = 1.9$					
30	9.9969	0.031	9.9965	0.035	10.0000
35	5.7192	0.025	5.7240	0.109	5.7177
40	3.2462	0.050	3.2506	0.183	3.2446
45	1.8600	0.051	1.8654	0.341	1.8591
50	1.0970	0.051	1.1041	0.696	1.0965
$\sigma = 0.3,\ \alpha = 1.9$					
30	10.5514	0.020	10.5600	0.102	10.5493
35	7.4364	0.038	7.4433	0.131	7.4336
40	5.2640	0.052	5.2717	0.197	5.2613
45	3.7580	0.058	3.7667	0.289	3.7558
50	2.7161	0.062	2.7265	0.445	2.7144
$\sigma = 0.1,\ \alpha = 1.8$					
30	10.0000	0.000	10.0000	0.000	10.0000
35	5.0000	0.000	5.0000	0.000	5.0000
40	1.4407	0.342	1.4423	0.457	1.4358
45	0.5496	0.174	0.5524	0.681	0.5486
50	0.2899	0.093	0.2922	0.881	0.2896
$\sigma = 0.2,\ \alpha = 1.8$					
30	9.9973	0.027	9.9924	0.076	10.0000
35	5.7891	0.065	5.7943	0.155	5.7854
40	3.4319	0.081	3.4369	0.227	3.4291
45	2.1143	0.077	2.1204	0.365	2.1126
50	1.3742	0.070	1.3818	0.621	1.3733
$\sigma = 0.3,\ \alpha = 1.8$					
30	10.5587	0.093	10.5696	0.196	10.5489
35	7.5198	0.128	7.5274	0.228	7.5102
40	5.4315	0.144	5.4399	0.299	5.4237
45	3.9960	0.146	4.0056	0.385	3.9902
50	3.0043	0.144	3.0155	0.519	2.9999

CPU time: LTM-HCI (5 s), LTM-GS (5 s), FDM (399 s)

Table 2 Convergence rates of the LTM-HCI method in N

N	$\sigma = 0.3,\ \alpha = 1.9$		$\sigma = 0.2,\ \alpha = 1.8$	
	Error	Rate	Error	Rate
99	1.2725e−001	1.1027	8.4962e−002	1.0004
199	5.8924e−002	1.0288	4.2256e−002	0.9855
399	2.8804e−002	1.0075	2.1289e−002	1.0190
799	1.4310e−002	0.9893	1.0492e−002	1.0158
1599	7.2034e−003	1.0021	5.1854e−003	0.9784
3199	3.5953e−003	–	2.6311e−003	–

The parameters are set as $\tau = 2,\ r = 0.05,\ K = 40,\ L = 6$

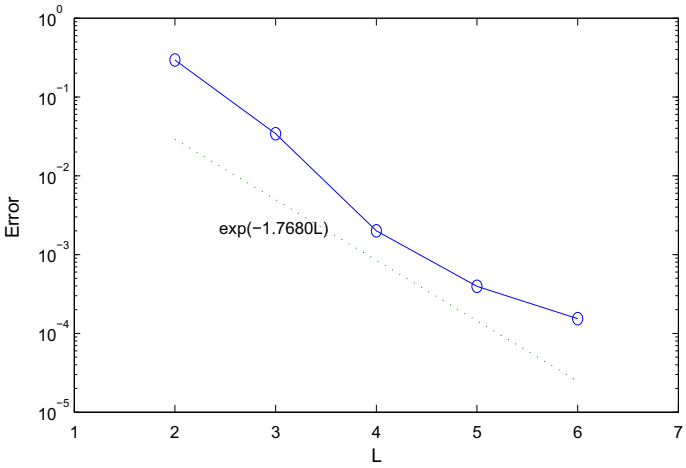

Fig. 4 LTM-HCI errors with different L, the *circle line* represents the computational error and the *dot line* the theoretical error. Parameters are taken as $\sigma = 0.3,\ \alpha = 1.9,\ K = 40,\ r = 0.05,\ \tau = 2$ and $N = 6999$

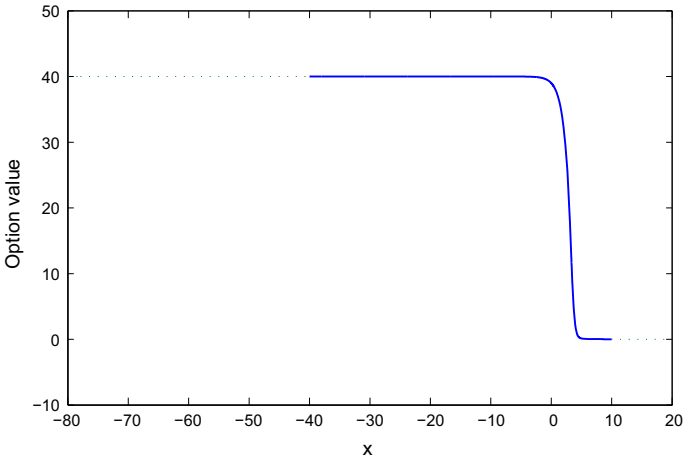

Fig. 5 LTM-HCI solution (option value) with different truncation x_L and x_R. Parameters are taken as $\sigma = 0.3,\ \alpha = 1.9,\ K = 40,\ r = 0.05,\ \tau = 2,\ L = 6$. The *solid line* represents the option value computed with $x_L = -40,\ x_R = 10$ and $N = 3999$, and the *dot line* the option value computed with $x_L = -80,\ x_R = 20$ and $N = 5999$

6 Conclusions

The Laplace transform method is regarded as a better alternative to the time-stepping method for solving PDEs or FPDEs. The Laplace transform method (or contour integral method) is much faster than the commonly used time-stepping method. The methods have been developed for fixed-boundary PDEs and FPDEs (see McLean and Thomée [19], Pang and Sun [24], and the references therein). But to the best of our knowledge, there is no significant breakthrough for the free-boundary problems of FPDEs. In fact there are several challenges in developing the methods for free-boundary FPDEs. This paper successfully developed a fast Laplace transform method for solving a class of free-boundary FPDEs. A hyperbola contour integral method was also developed for the fast Laplace inversion. Numerical results showed that the fast Laplace methods are faster than the time-stepping methods.

Compliance with Ethical Standards

Conflict of interest None.

References

1. Ahna, J., Kang, S., Kwonc, Y.: A Laplace transform finite difference method for the Black–Scholes equation. Math. Comput. Model. **51**, 247–255 (2010)
2. Cai, N., Kou, S.G.: Option pricing under a mixed-exponential jump diffusion model. Manag. Sci. **57**, 2067–2081 (2011)
3. Cai, N., Kou, S.G.: Pricing Asian options under a hyper-exponential jump diffusion model. Oper. Res. **60**, 64–77 (2012)
4. Carr, P.: Randomization and the American put. Rev. Financ. Stud. **11**, 597–626 (1998)
5. Carr, P., Wu, L.: The finite moment log stable process and option pricing. J. Financ. **58**, 597–626 (2003)
6. Chan, R., Jin, X.: An Introduction to Iterative Toeplitz Solvers. SIAM, Philadelphia (2007)
7. Chen, W., Xu, X., Zhu, S.P.: Analytically pricing European-style options under the modified Black–Scholes equation with a spatial-fractional derivative. Q. Appl. Math. **72**, 597–611 (2014)
8. Chen, X.F., Chadam, J.: A mathematical analysis of the optimal exercise boundary for American put options. SIAM J. Math. Anal. **38**, 1613–1641 (2006)
9. Davydov, D., Linetsky, V.: Pricing and hedging path dependent options under the CEV process. Manag. Sci. **47**, 949–965 (2001)
10. Horn, R., Johnson, C.: Topics in Matrix Analysis. Cambridge University Press, Cambridge (1991)
11. in't Hout, K.J., Weideman, J.A.C.: A contour integral method for the Black–Scholes and Heston equations. SIAM J. Sci. Comput. **33**, 763–785 (2011)
12. Kimura, T.: Valuing finite-lived Russian options. Eur. J. Oper. Res. **189**, 363–374 (2008)
13. Lee, H., Sheen, D.: Laplace transformation method for the Black–Scholes equation. Int. J. Numer. Anal. Model. **6**, 642–658 (2009)
14. Lee, H., Sheen, D.: Numerical approximation of option pricing model under jump diffusion using the Laplace transformation method. Int. J. Numer. Anal. Model. **8**, 566–583 (2011)
15. Lee, H., Lee, J., Sheen, D.: Laplace transform method for parabolic problems with time dependent coefficients. SIAM J. Numer. Anal. **51**, 112–125 (2013)
16. Lee, S., Pang, H., Sun, H.: Shift-invert Arnoldi approximation to the Toeplitz matrix exponential. SIAM J. Sci. Comput. **32**, 774–792 (2010)
17. Leippold, M., Vasiljević, N.: Pricing and disentanglement of American puts in the hyper-exponential jump-diffusion model. http://ssrn.com/abstract=2571208 (2015)
18. McLean, W., Sloan, I.H., Thomée, V.: Time discretization via Laplace transformation of an integro-differential equation of parabolic type. Numer. Math. **102**, 497–522 (2006)
19. McLean, W., Thomée, V.: Time discretization of an evolution equation via Laplace transformation. IMA J. Numer. Anal. **24**, 439–463 (2004)
20. McLean, W., Thomée, V.: Numerical solution via Laplace transformation of a fractional order evolution equation. J. Integral Equ. Appl. **22**, 57–94 (2010)

21. McLean, W., Thomée, V.: Maximum-norm error analysis of a numerical solution via Laplace transformation and quadrature of a fractional-order evolution equation. IMA J. Numer. Anal. **30**, 208–230 (2010)
22. Meerschaert, M.M., Tadjeran, C.: Finite difference approximations for fractional advection–diffusion flow equations. J. Comput. Appl. Math. **172**, 65–77 (2004)
23. Meerschaert, M.M., Tadjeran, C.: Finite difference approximations for two-sided spacefractional partial differential equations. Appl. Numer. Math. **56**, 80–90 (2006)
24. Pang, H., Sun, H.: Fast numerical contour integral method for fractional diffusion equations. J. Sci. Comput. **66**, 41–66 (2016)
25. Pelsser, A.: Pricing double barrier options using Laplace transform. Financ. Stochast. **4**, 95–104 (2000)
26. Podlubny, I.: Fractional Differential Equations. Academic press, New York (1999)
27. Pun, C.S., Wong, H.Y.: CEV asymptotics of American options. J. Math. Anal. Appl. **403**, 451–463 (2013)
28. Sepp, A.: Analytical pricing of double barrier options under a double-exponential jump diffusion process: applications of Laplace transform. Int. J. Theor. Appl. Financ. **7**, 151–175 (2004)
29. Sheen, D., Sloan, I.H., Thomée, V.: A parallel method for time discretization of parabolic problems based on contour integral representation and quadrature. Math. Comput. **69**, 177–195 (1999)
30. Sheen, D., Sloan, I.H., Thomée, V.: A parallel method for time discretization of parabolic equations based on Laplace transformation and quadrature. IMA J. Numer. Anal. **23**, 269–299 (2003)
31. Stehfest, H.: Numerical inversion of Laplace transforms. Commun. ACM **13**, 47–49 (1970)
32. Talbot, A.: The accurate numerical inversion of Laplace transforms. J. Inst. Math. Appl. **23**, 97C120 (1979)
33. Tilli, P.: Singular values and eigenvalues of non-Hermitian block Toeplitz matrices. Linear Algebra Appl. **272**, 59–89 (1998)
34. Weideman, J.A.C.: Improved contour integral methods for parabolic PDEs. IMA J. Numer. Anal. **30**, 334–350 (2010)
35. Weideman, J.A.C., Trefethen, L.N.: Parabolic and hyperbolic contours for computing the Bromwich integral. Math. Comput. **76**, 1341–1356 (2007)
36. Wong, H.Y., Zhao, J.: Valuing American options under the CEV model by Laplace–Carson trnsforms. Oper. Res. Lett. **38**, 474–481 (2010)
37. Xu, M., Knessl, C.: On a free boundary problem for an American put option under the CEV process. Appl. Math. Lett. **24**, 1191–1198 (2010)
38. Zhu, S.P.: A new analytical approximation formula for the optimal exercise boundary of the American put options. Int. J. Theor. Appl. Financ. **7**, 1141–1177 (2006)